

# Investigation of Ultrathin Films of Processable Poly(*o*-anisidine) Conducting Polymer Obtained by the Langmuir–Blodgett Technique

Sergio Paddeu,<sup>†,§</sup> Manoj K. Ram,<sup>‡</sup> and Claudio Nicolini<sup>\*,†</sup>

*Institute of Biophysics, School of Medicine and Surgery, University of Genoa, Via Giotto 2, 16153 Genova, Italy, and E.L.B.A. Foundation, Viale Marconi 893, 00146 Roma, Italy*

*Received: October 10, 1996; In Final Form: March 1, 1997<sup>®</sup>*

Langmuir films of poly(*o*-anisidine) conducting polymer in its undoped (emeraldine base) and doped (emeraldine salt) forms have been obtained by the proper selection of subphase.  $\pi/A$  isotherms, quartz crystal microbalance, Brewster angle microscopic, and UV–vis–near IR spectroscopic measurements provided evidence concerning the effects of HCl doping on the polymer molecular organization as well as film properties. The analysis underlines that the presence of dopant induces structural and conformational changes on the polymer structure from the emeraldine base to emeraldine salt, so causing a different arrangement of the molecules at the air/water interface. Moreover, the emeraldine base form of poly(*o*-anisidine) Langmuir films evidenced less compressibility, as suggested by the presence of aggregates at high surface pressures, and a lower collapse surface pressure with respect to the emeraldine salt one. The investigation of the Langmuir film formation by the Brewster angle microscopy made it possible to support the previous experimental results and to image directly two (2D)–three (3D) dimensional transformations, which occurred by overcompressing beyond the limiting densities of close-packed 2D films, namely, collapse pressure. The recorded optical spectra revealed the development of polarons and bipolarons due to inclusion of the dopant in the polymer backbone and also provided an estimation of the poly(*o*-anisidine) bandgap.

## Introduction

Among the conjugated conducting polymers,<sup>1–3</sup> the polyaniline<sup>4–9</sup> has been widely investigated aiming toward potential applications for rechargeable batteries,<sup>10</sup> electrochromic displays, memory storage and molecular electronic devices,<sup>11</sup> biosensors,<sup>12,13</sup> membranes,<sup>14</sup> corrosion protection,<sup>15</sup> and electronic and optical devices.<sup>16–18</sup> Still, processability is a heralding problem in the commercial exploitation of polyaniline.<sup>18</sup> In this regard, efforts have been made to increase the processability using the various substituent groups (–CH<sub>3</sub>, –OCH<sub>3</sub>, –OC<sub>2</sub>H<sub>5</sub>, etc.) in the polymer backbone<sup>19–25</sup> (Figure 1a). Therefore, in recent years substituted polyanilines such as poly(*o*-anisidine) (POAS),<sup>25,26</sup> poly(methylaniline),<sup>21,23,24</sup> or poly(*o*-alkoxyaniline)<sup>22</sup> have been synthesized showing the change in electron localization, redox kinetic, with an excellent solubility and a small decrease in conductivity in comparison to the parent polyaniline. Such substituted polyanilines increase the possibilities of adopting various techniques to fabricate conducting polymer thin films appropriate for several technologies as well as electronic and optical devices, coatings or sensors.<sup>27</sup> One of the techniques which makes it possible to obtain ultrathin films is the Langmuir–Blodgett (LB) method.<sup>27–29</sup> Although restricted to amphiphilic molecules, LB films have gained new attention justified by the trend in using new materials and molecular devices. This technique allows the organization of the molecules in a monolayer at a gas/liquid interface and then to transfer it onto a solid support in a controlled way. LB films of such substituted polyanilines have been fabricated, also enabling them to characterize the conducting polymer at a molecular level when organized into an ultrathin film.<sup>19,22,25</sup> Among substituted polyanilines, POAS LB films can be considered to be in an important class due to their optical and

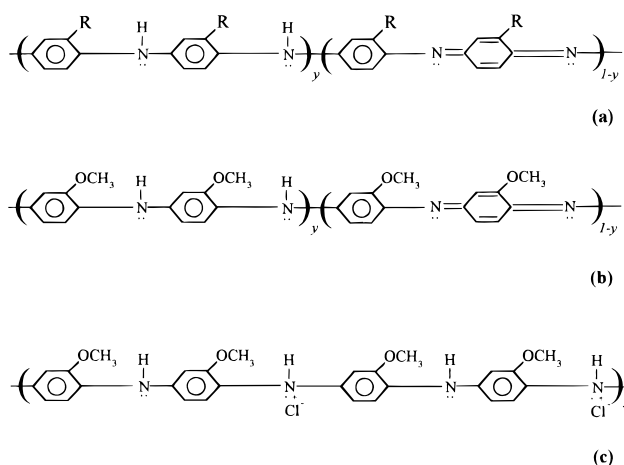


**Figure 1.** Structures of polymer repeating unit: (a) base form of polyaniline in the emeraldine oxidation state; (b) POAS emeraldine base; (c) emeraldine salt.

electrical properties.<sup>25,26</sup> In fact, the conductivity of POAS, like polyaniline, depends upon the oxidation state of the main chain and the degree of protonation of nitrogen atoms in the polymer backbone.<sup>2,4–6</sup> The doping yields different structures from the emeraldine base (EB) to emeraldine salt (ES) forms of POAS as shown in Figure 1b,c. Therefore, it is necessary to understand the organization of polymer molecules when assembled into ultrathin film and to know the features of the film itself.

Beginning with these considerations, the principle aim of this work was to analyze the formation and the deposition of POAS ultrathin films obtained by the Langmuir–Blodgett technique, as well as to investigate the effect of the HCl doping process occurring in the formation of Langmuir films, as regards the organization of the polymer molecules and the inclusion of the dopant in the polymer backbone structure.

POAS LB films were first studied at the air/water interface by the analysis of the  $\pi/A$  isotherms and by the Brewster angle microscopy (BAM).<sup>30–32</sup> This microscopy allowed one to image

<sup>†</sup> University of Genoa.

<sup>‡</sup> E.L.B.A. Foundation.

<sup>§</sup> e-mail: paddeu@ibf.unige.it.

<sup>®</sup> Abstract published in *Advance ACS Abstracts*, June 1, 1997.

directly the morphology and the 2D–3D transformations<sup>29</sup> of the film which occur during its formation. The formed films were deposited onto a solid support by the Langmuir–Schaefer method<sup>33</sup> and subsequently studied by a quartz crystal microbalance (QCM)<sup>34,35</sup> and by a UV–vis–near-IR spectroscopy. The features of these POAS thin films, such as stability at the air/water interface, the reliability of the deposition or the optical properties, have been studied according to the doped state of the polymer, i.e., emeraldine base and emeraldine salt forms.

## Experimental Section

**Polymer Synthesis.** *o*-Anisidine monomer, oxidizing agents, and reagents of analytical grade were purchased from the Sigma Chemical Co. Poly(*o*-anisidine) conducting polymer was chemically synthesized<sup>2,25,36,37</sup> by oxidative polymerization of *o*-anisidine monomer using ammonium perdisulfate [(NH<sub>4</sub>)<sub>2</sub>S<sub>2</sub>O<sub>8</sub>] under controlled conditions. *o*-Anisidine (27 mL, 0.219 M) was added to a 1 M HCl solution and cooled to 0–4 °C. Ammonium perdisulfate (11.5 g, 0.05 M) was dissolved in the 1 M HCl solution and also cooled separately to 0–4 °C. Then the precooled ammonium perdisulfate in HCl was slowly added to the *o*-anisidine solution, and the reaction was continued for a further 12 h in similar conditions by stirring. POAS precipitate, dark green in color, was recovered from the reaction vessel and subsequently filtered and washed with 1 M HCl. This step allowed the removal of the oxidant and oligomers. The precipitate was then washed several times with deionized water and methanol and diethyl ether, to remove the polymers with low molecular weight as well. The emeraldine form of POAS was then heated at 100 °C, and the dark green powder obtained is POAS ES. Such ES of POAS was then treated with aqueous ammonia for 24 h, washed several times with distilled water and acetone, and finally dried for 6 h at 100 °C. Therefore a dark blue powder was obtained; this is the EB of POAS conducting polymer.

**Film Formation and Deposition.** Langmuir films of POAS were formed in a Langmuir–Blodgett trough with a surface area of 24 × 10 cm<sup>2</sup> (MDT Corp., Moscow, Russia) measuring the surface pressure by a Wilhelmy balance having an accuracy of 0.2 mN m<sup>-1</sup>. POAS emeraldine base powder was dissolved in pure chloroform to a final concentration of 0.2 mg mL<sup>-1</sup> and then sonicated to obtain a homogeneous polymer stock solution. The spread amount of this stock solution was varied in the range 40–200 μL; 2 min elapsed before compressing the film, to allow for the evaporation of chloroform. The compression of the film was performed at a speed of 100 cm<sup>2</sup> min<sup>-1</sup>. The utilized subphases for the Langmuir film formation were started with pure water (pH 6.8) and was changed to HCl acidified solution (up to pH 1) in order to form POAS EB and POAS ES LB films, respectively. The change in pH affects the concentration of ions (H<sup>+</sup> and Cl<sup>-</sup>) in the solution. When the pH is within the range 1–3, the molar concentration is lying in the range (0.06–0.5) × 10<sup>-4</sup> M; when the pH is between 4 and 5.27, the molarity of the solution is lying between 0.2 × 10<sup>-5</sup> and 10<sup>-7</sup> M. As it is well-known that a higher doping level in polyanilines is achieved with lower pH,<sup>4–6</sup> a HCl-acidified solution at pH 1 was finally considered in order to analyze the doped form of POAS LB films. The Langmuir films were transferred onto solid supports using the Langmuir–Schaefer method (horizontal lifting).<sup>33</sup> Quartz and glass plates were used as solid support.

**Film Characterization.** (a) *Gravimetric Analysis.* Gravimetric measurements were carried out using a quartz crystal microbalance (QCM)<sup>34,35</sup> utilizing 10 MHz quartz resonators according to the procedure shown in literature.<sup>38</sup> A POAS layer was deposited on both sides of the resonator and dried with a

nitrogen flux, and then the frequency shift due to the film deposition was registered. By means of this technique, it was possible to estimate the surface density and the area per repeating unit (ru) values by depositing the Langmuir–Blodgett film at different surface pressures, as well as the reliability of the deposition itself.

(b) *Brewster Angle Microscopy.* The Brewster angle microscopy (BAM)<sup>30–32</sup> offers the opportunity of imaging a monolayer directly at the air/water interface (or more generally at a gas/liquid interface) without employing any fluorescent probe. This microscopy allows one to investigate the formation and the morphology of a Langmuir film as well as its anisotropy.<sup>39–41</sup> The POAS Langmuir film formation was analyzed with a BAM2 Brewster angle microscope (Nanofilm Technologie GmbH, Göttingen, Germany), coupled with a NIMA LB trough (NIMA, England, type 601; surface pressure sensor type PS3), by spreading 200 μL of the stock solution (0.2 mg mL<sup>-1</sup>) at the air/water interface and by compressing the film according to the previously described procedure. The p-polarized beam light from a laser diode (λ = 690 nm, 30 mW) was incident at the Brewster angle (53.1°)<sup>42</sup> to the air/water interface. Under such conditions of incidence, the reflectivity of the water surface was minimized. The beam, reflected in the presence of the insoluble POAS film (i.e., the Brewster conditions are modified), was imaged by a CCD camera and recorded by means of a video recorder. BAM images were acquired during the continuous film compression simultaneously with the π/A isotherm. The lateral resolution was about 2 μm and the digitized images were 420 μm × 630 μm (512 × 768 pixels) in size.

(c) *UV–vis–Near-IR Spectroscopy.* Optical properties of POAS LB films, in doped (ES) and undoped (EB) forms, were analyzed with an UV–vis–near-IR double-beam spectrophotometer (Jasco 7800, Japan). The spectra were recorded in the range 200–1100 nm (6.2–1.12 eV). The POAS LB films were deposited onto a quartz plate at a surface pressure of 25 mN m<sup>-1</sup> and were 20 layers thick. Absorption optical spectra allowed the assess of the inclusion of dopant in the polymer backbone in addition to evaluating the bandgap.<sup>2,3</sup> The bandgap, whose width determines the electrical and the optical properties of the polymer, was estimated as shown in the literature.<sup>2</sup>

## Results and Discussion

**Analysis at the Air/Water Interface.** Poly(*o*-anisidine) was finally obtained in its undoped form, which is called the emeraldine base. Its repeating unit structure is shown in Figure 1b. The adopted synthesis<sup>2,36,37</sup> made it possible to obtain a processable polymer,<sup>2,25</sup> which showed a high solubility degree in organic solvents such as chloroform, which was then chosen to dissolve the polymer powder to obtain the stock solution. It is known that the doping process is able to affect the electrooptical properties of the polymer,<sup>3</sup> changing its structure,<sup>2</sup> and that there are different doping processes<sup>2</sup> as well as dopants. In this work the doped polymer organized in the LB film was obtained by forming the Langmuir film on HCl-acidified subphases. The possibility of forming Langmuir films of POAS was proved by the recorded π/A isotherms.<sup>25</sup> Therefore, the effect of subphase on Langmuir films of POAS conducting polymer was systematically analyzed by carrying out π/A isotherms at a different pH of subphase. Figure 2 shows such isotherms: curve a is related to pure water (pH 6.8) while curves b–f are referred to as HCl-acidified solutions, from pH 5 to pH 1. By decreasing the pH solution (i.e., increasing the dopant concentration or the molarity of solution), it was possible to observe that the polymer molecules were arranged in a different way at the air/water interface, as suggested by the decrease of

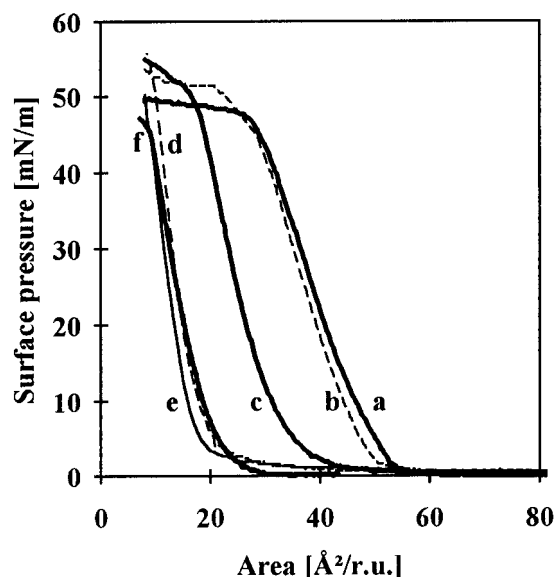


**Figure 2.**  $\pi/A$  isotherms of POAS Langmuir films obtained by proper selection of subphase: (a) pure water; (b–f) from pH 5 to pH 1 (step 1) by HCl acidification of solution.

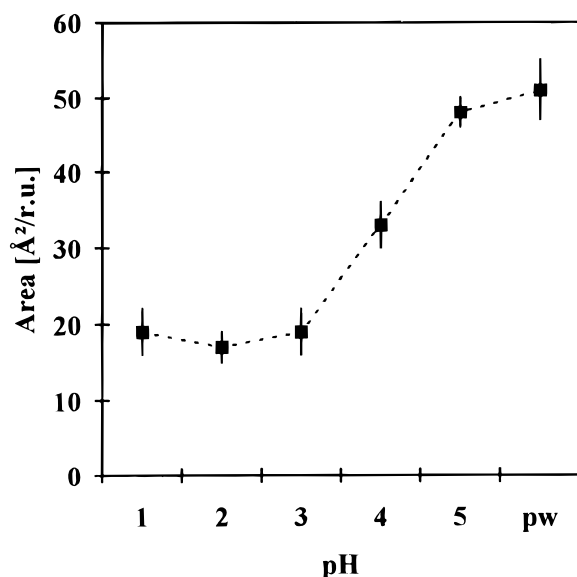


**Figure 3.** Estimation of the occupied area per repeating unit (ru) of POAS polymer at the air/water interface when organized in a Langmuir film. The values have been evaluated by analyzing the  $\pi/A$  isotherms.

the occupied area per repeating unit (ru).<sup>25</sup> In fact, an attempt was made to estimate the area per molecule of POAS at the air/water interface directly from the  $\pi/A$  isotherm.<sup>29</sup> This estimation was carried out taking into account one repeating unit of POAS polymer (molecular weight  $\approx 480 \text{ g mol}^{-1}$ ) as shown in Figure 1b.

Figure 3 shows the area per ru of POAS in the condensed phase at the air/water interface and refers to the two-dimensional (2D) transformations,<sup>29</sup> as a function of a different pH of subphase. It appeared that at high pH, up to 5 (i.e. very low dopant concentration), the area was estimated to be in the range 48–55  $\text{\AA}^2/\text{ru}$  and that the low doping agent concentration did not highly affect the organization of the polymer chain structure at the air/water interface with respect to that estimated with pure water. When the film was formed at low pH, up to pH 1, the polymer chain was arranged differently and/or oriented and highly affected by the inclusion of the dopant (Figure 1c), as confirmed by the lowest area per ru whose value was in the range 18–24  $\text{\AA}^2/\text{ru}$ . This last value is close to the expected area of the aniline monomer.<sup>43,44</sup> This decrease of the area per

ru, by increasing the molar concentration of the dopant, is ascribable to a different molecular arrangement at the air/water interface.

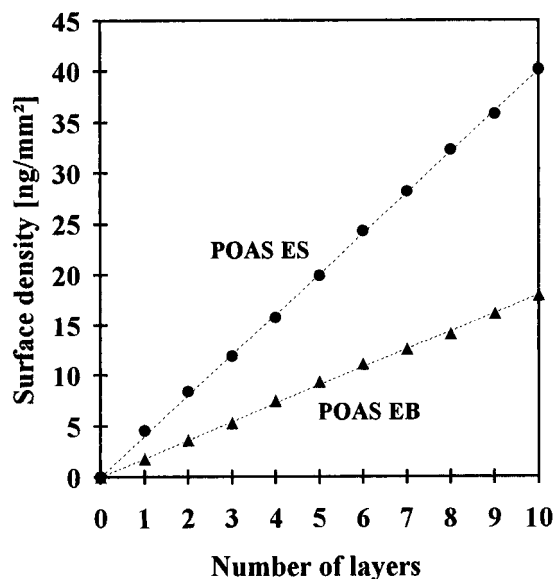
Taking into account these results, the investigation was restricted to the undoped form (i.e., utilizing pure water as a subphase) and to the highest reachable doped form (i.e., adopting a HCl-acidified solution at pH 1 as subphase) of POAS LB films. With a detailed analysis of undoped film formation, it was possible to observe that an initial increase of the surface pressure took place compressing the Langmuir film near to 55–60  $\text{\AA}^2/\text{ru}$  (Figure 2a). From this point a smooth phase transition was visible, and subsequently a pronounced increase in the surface pressure was recorded. During this phase the polymer molecules starts to interact closely, thus increasing the 2D packing degree. When a surface pressure of 40  $\text{mN m}^{-1}$  was reached, the film began to collapse as suggested by the isotherm and by the aggregates at the interface visible even with the naked eye. This fact indicated that a 2D–3D transformation took place.<sup>29,45</sup> A further compression of the Langmuir film underlined a plateau approach up to 45–53  $\text{mN m}^{-1}$  and an increase in the 3D transformations (collapses). This behavior indicated two phase transitions as well as a different packing degree of polymer molecules at the air/water interface during the POAS EB Langmuir film formation. The area per ru from the  $\pi/A$  isotherm was estimated to be about 50  $\text{\AA}^2/\text{ru}$ .<sup>25</sup> It reveals that the orientation and/or the arrangement at the air/water interface of POAS conducting polymer is much more different than that of the parent polyaniline<sup>44,45</sup> due to the presence of the methoxy group in the polymer backbone.

The  $\pi/A$  isotherm of POAS Langmuir film at a subphase of pH 1 (Figure 2f) underlined a pattern similar to that observed with pure water. The surface pressure started to increase in a smoother way up to a pressure of 10  $\text{mN m}^{-1}$ , from the range 25–30  $\text{\AA}^2/\text{ru}$ . The surface pressure increased sharply from this value approximately up to 45  $\text{mN m}^{-1}$ . A further compression of the film causes a plateaulike behavior of the surface pressure. Although this fact suggested that the film begins to collapse near 45  $\text{mN m}^{-1}$ , no aggregates were visible with the naked eye as in the previous case. This emphasized that despite the 2D–3D transformation which occurred, the film showed a higher compressibility in comparison with that of the undoped one. The average area per ru was estimated to be 20  $\text{\AA}^2/\text{ru}$ . As far as the molecular area at pH 1 is concerned, it is much more different than the EB of POAS but agrees well with the area occupied by one repeat unit of polyaniline molecules at the air/water interface.<sup>43,44</sup> These experimental observations suggested that the dopant ions induced a molecular organization for each aniline-substituted group. Therefore, the presence of dopant in the subphase caused structural changes of the POAS molecules, thus inducing a different orientation and/or organization of the polymer at the air/water interface. It is well-known that the doping process affects the polymer molecule structure causing structural and conformational changes due to a different charge distribution<sup>2</sup> in the backbone.

Moreover, with regard to the presence of dopant, an analysis was carried out at the air/water interface to evaluate the stability of the film. A noted fact is that part of the defects in the deposited films is formed already at the air/water interface.<sup>45</sup> Therefore, the stability of the film at constant deposition pressures can be crucial for the preparation of ordered layered structures of low concentrations of defects. This parameter is related to the Langmuir films and can be defined as the percentage decrease of film area in comparison with its initial value at a fixed surface pressure. The study was carried out at different surface pressures considering the isotherms. The results are summarized in Table 1. The stability of both films

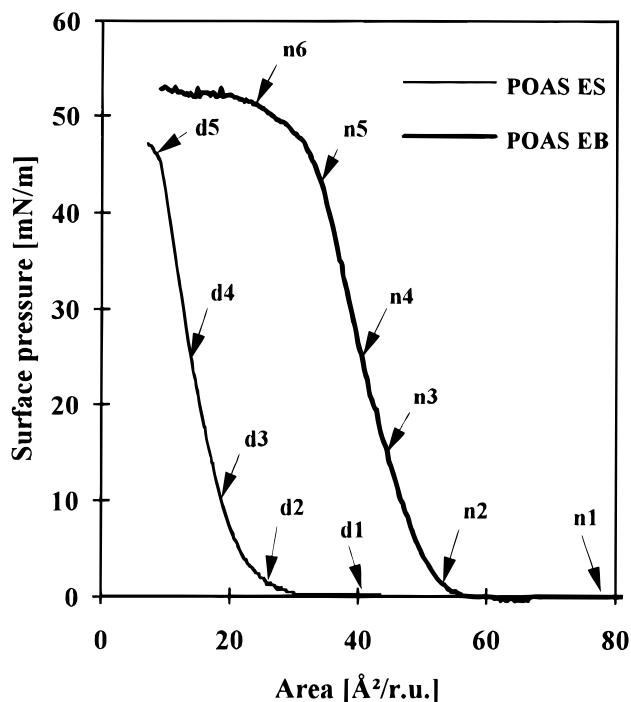
**TABLE 1: Summary of the Main Features of POAS Polymer Organized in Ultrathin Film Using the Langmuir–Blodgett Technique**

	surface pressure (mN m <sup>-1</sup> )	POAS EB form	POAS ES form
stability of the Langmuir film	25	≈2% min <sup>-1</sup>	≈2.6% min <sup>-1</sup>
	45	≈6% min <sup>-1</sup>	≈3% min <sup>-1</sup>
area per ru <sup>a</sup>	15	50 ± 5 Å <sup>2</sup> /ru	25 ± 3 Å <sup>2</sup> /ru
surface density		1.6 ± 0.16 ng mm <sup>-2</sup>	3.27 ± 0.39 ng mm <sup>-2</sup>
	25	45 ± 5 Å <sup>2</sup> /ru	20 ± 3 Å <sup>2</sup> /ru
		1.79 ± 0.19 ng mm <sup>-2</sup>	4.01 ± 0.6 ng mm <sup>-2</sup>
	35	42 ± 4 Å <sup>2</sup> /ru	19 ± 3 Å <sup>2</sup> /ru
		1.9 ± 0.18 ng mm <sup>-2</sup>	4.3 ± 0.6 ng mm <sup>-2</sup>
	45	38 ± 4 Å <sup>2</sup> /ru	15 ± 2 Å <sup>2</sup> /ru
		2.12 ± 0.22 ng mm <sup>-2</sup>	5.25 ± 0.7 ng mm <sup>-2</sup>
area per ru <sup>b</sup>		52 ± 3 Å <sup>2</sup> /ru	20 ± 3 Å <sup>2</sup> /ru
optical peaks		315 nm (3.93 eV)	352 nm (3.52 eV)
		619 nm (2.0 eV)	450 nm (2.75 eV)
			870 nm (1.42 eV)
bandgap		≈3.8 eV	≈2.7 eV
conductivity <sup>c</sup>		10 <sup>-10</sup> S cm <sup>-1</sup>	0.1 S cm <sup>-1</sup>
color		blue	dark green

<sup>a</sup> Results obtained by QCM analysis. <sup>b</sup> Estimated by  $\pi/A$  isotherms.<sup>c</sup> As order of magnitude.**Figure 4.** Increase of surface density vs number of layers: after each film deposition the frequency shift of the resonator is registered and then suitably converted. The curves shown are related to the films deposited at 25 mN m<sup>-1</sup>.

(i.e., POAS EB and POAS ES LB films) at 25 mN m<sup>-1</sup> were comparable and closer to 2% min<sup>-1</sup>, whereas the film at 45 mN m<sup>-1</sup> showed more differences due to the strong increment of collapses in the undoped POAS LB film.

Together with the stability of the Langmuir film, it was possible to support the choice of surface deposition pressure carrying out a gravimetric analysis with a QCM.<sup>38</sup> The study was performed by depositing the POAS EB and the POAS ES LB films on quartz resonators at a pressure in the range 15–45 mN m<sup>-1</sup>. The results underlined that the deposition was generally reliable within an average percentage error of about 10–15%, with a small variation depending on the considered deposition pressure. In Figure 4 a typical increase in surface density due to each film deposition at the surface deposition pressure of 25 mN m<sup>-1</sup> is shown. The surface density strongly changed from the POAS EB to the POAS ES form as summarized in Table 1. The presence of dopant increased the surface density: it was possible to refer this change to the protonation process which determines the inclusion of the chloride counterion and caused polymer conformational changes.<sup>2</sup>

**Figure 5.**  $\pi/A$  isotherms of POAS EB (thick line) and of POAS ES (thin line) LB films. Each arrow indicates the value of surface pressure at which the BAM images of Figures 6–8 were acquired. The shape of the isotherms was correlated to the 2D–3D transformations which occurred to the POAS Langmuir film.

In addition, a decrease in the area per ru (see Table 1) revealed once more that the POAS polymer was subjected to such a process which then organized the molecules in the LB film in a different way. The obtained area per ru values were in agreement with those estimated analyzing the  $\pi/A$  isotherms, thus confirming that the previous evaluation by the isotherms was reliable. Furthermore, these facts also suggest that the molecules in the film could not be subjected to a strong reorganization after the film deposition.<sup>29</sup>

**Brewster Angle Microscopy.** The Langmuir film formation was then imaged and analyzed by means of a BAM. It was also possible to detect film inhomogeneities and breaks as well as the 2D–3D transformations which occurred at different surface pressures. These features were then considered on a merit factor to establish the best deposition pressure range. The recorded  $\pi/A$  isotherms of the POAS EB and the POAS ES LB film are shown in Figure 5: each arrow indicates the surface pressure at which the BAM image was acquired.

Typical morphologies related to the investigation carried out on POAS EB Langmuir films are shown in the images summarized in Figure 6. Small domains subjected to a laminar motion immediately after spreading and before compression were visible (image n1;  $\pi \approx 0$  mN m<sup>-1</sup>). When compression started, at very low surface pressures (image n2;  $\pi \approx 2$  mN m<sup>-1</sup>), the film began to form domains in which the molecular density increased smoothly up to 3–5 mN m<sup>-1</sup> visible with the isotherm as well. Exceeding this surface pressure the film morphology changed, giving prominence to big domains (condensed phase), where the molecular packing degree increased (images n3 and n4). This increase in molecular interaction can be referred to as 2D transformations.<sup>29,45</sup> In fact, it was possible to observe that the film was rather uniform with small defects or breaks, the presence of which statistically decreased, increasing the surface pressure to less than the value of 40 mN m<sup>-1</sup>. While 3D transformations, like aggregates, were visible exceeding the surface pressure of 40 mN m<sup>-1</sup>. These events refer to collapses of the film (image n5).<sup>29</sup> Further

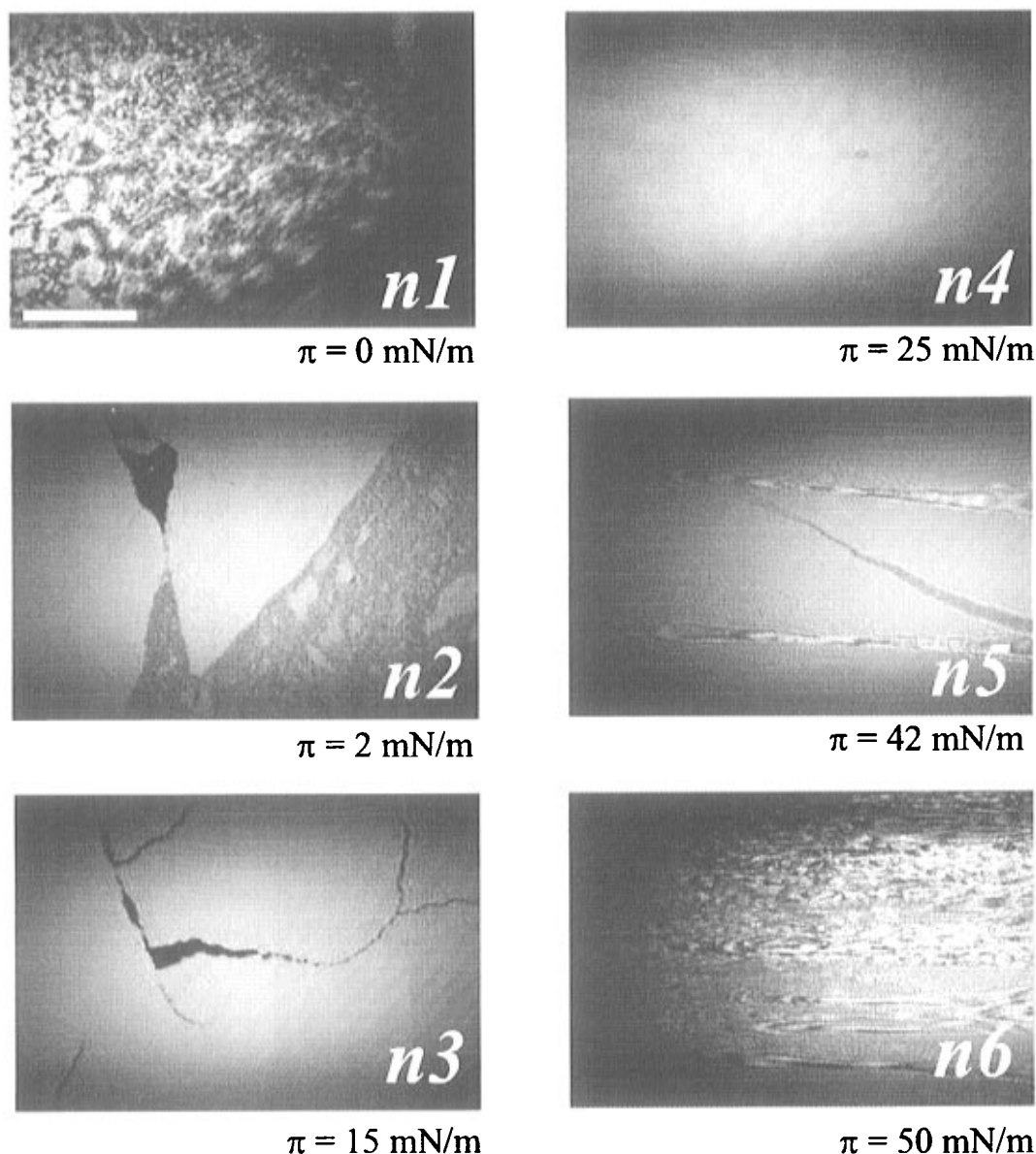


**Figure 6.** BAM images obtained during formation of the POAS EB Langmuir film utilizing pure water at subphase. The considered sequence of images displays the typical 2D–3D transformations that occur during the continuous compression of the film. Images n5 and n6 show the irreversible 3D transformations, such as the overlapping of the film or the growth of crystal aggregates, which occur overcoming the surface pressure of 40 mN m<sup>-1</sup> and are referred to as collapses of the film. The value near each image indicates the surface pressure at which it was acquired. The bar represents 150 μm.

increase of surface pressure caused an increase in their density (image n6). In fact, these transformations lead to an overlapping or aggregation of the Langmuir film, which determines the growth of 3D structures and disturbs the homogeneity and the integrity of the deposited film, so causing in-plane discontinuities and possible rearrangement of the LB film formed by multilayers. As visible with the isotherm, the above 3D transformations corresponded to a strong overcompression of the film and determined a plateaulike behavior of surface pressure. In these conditions the film showed massive 3D structures which were also visible with the naked eye, as already stated.

Furthermore, it is worth noting that the opening of barriers, when the maximum compression is reached, led to a complete break in the film with a sharp surface pressure transition, which drops to 0 mN m<sup>-1</sup>. Figure 8 (image a1 and a2) shows that the collapses formed at high surface pressures were still present, thus indicating that these 3D transformations are irreversible.

The morphological 2D–3D transformations of doped POAS Langmuir films obtained at pH 1 were imaged as in the undoped case. The typical morphologies which occurred during the

POAS ES film formation are summarized in the BAM images of Figure 7. Immediately after the spreading operation, the POAS polymer appears to be organized in a film (image d1), thus not showing an evident formation of small domains such as in the previous case. Film inhomogeneities were visible as domains of different gray level.<sup>39–41</sup> It is possible to assess that this appearance was caused directly by the presence of the doping agent which induce a dissimilar organization of the polymer molecules at the air/water interface. When the compression started, these inhomogeneities began to decrease (images d2 and d3), reflecting the shape of the recorded isotherm and underlying the increase of the molecular interactions. In fact, exceeding the surface pressure of 20 mN m<sup>-1</sup> the monolayer appeared more uniform (image d4), although the domains did not completely disappear and the presence of breaks was statistically lower. These results were in accordance with those obtained by the performed QCM analysis. Therefore, the morphology visible through the BAM underlined that high surface pressures, including those in the range 20–40 mN m<sup>-1</sup>, were suitable to have uniform 2D films. The first presence of

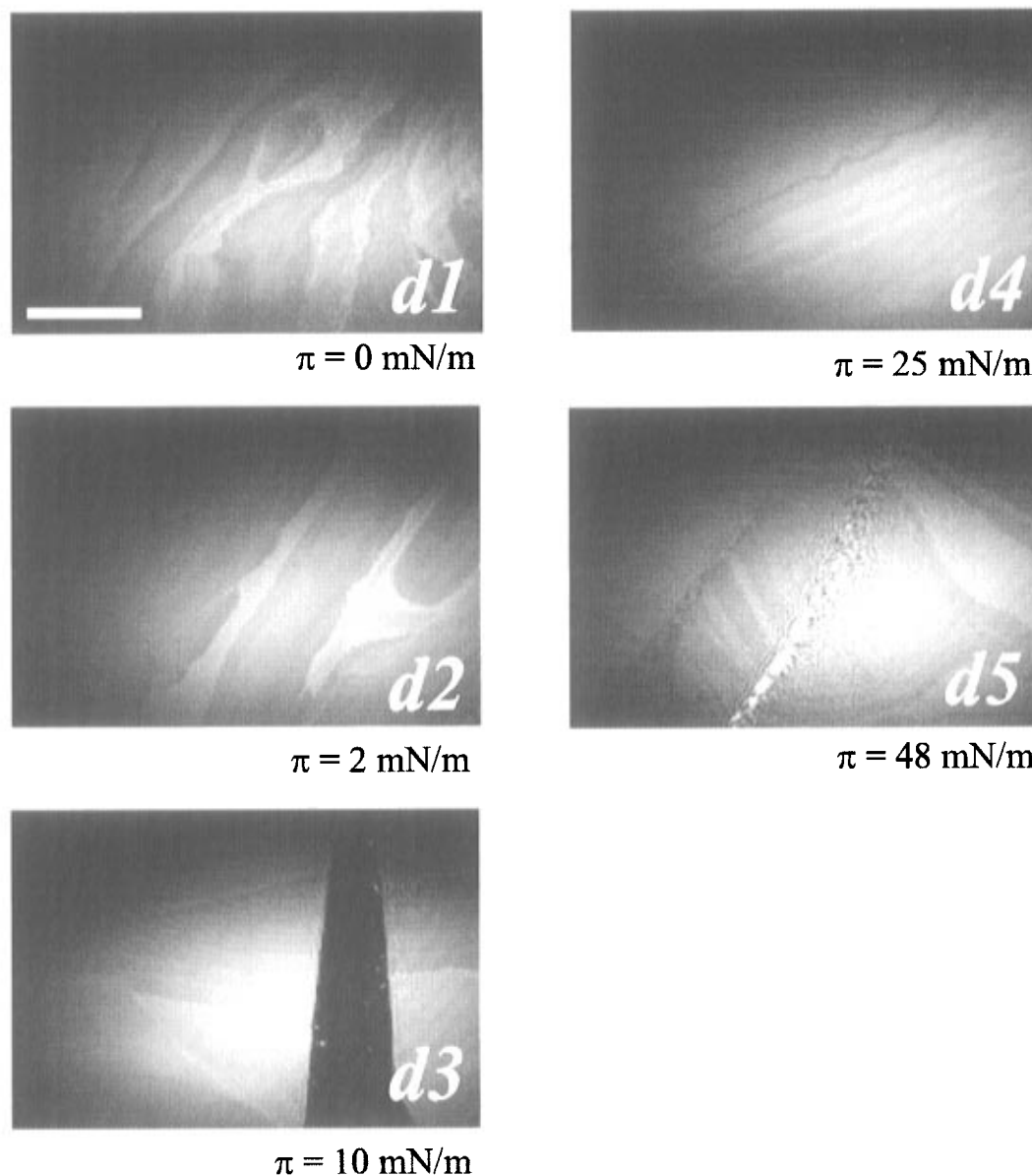


**Figure 7.** BAM images acquired during the formation of POAS ES Langmuir film at pH 1 of the subphase (acidification by HCl). The images display the 2D transformations and reveal the presence of film inhomogeneities induced by the dopant. At high surface pressures (image d5) it was possible to observe the 3D transformations, namely, the film collapses.

collapses or 3D transformations was detected exceeding the value of  $45 \text{ mN m}^{-1}$  of pressure (image d5). It was very interesting to observe that these 3D transformations did not occur harshly as in the undoped case, i.e., overcompressing the Langmuir film in which the presence of these irreversible processes was less although a plateau was attained (see the isotherm of Figure 5). Therefore the BAM analysis allowed one to support the previous analysis carried out directly at the air/water interface with simultaneous monitoring of the Langmuir film morphology.

As in the previous case, a sharp decrease in the surface pressure ( $\pi = 0 \text{ mN m}^{-1}$ ) opening the barriers was seen. This behavior indicated the fracture of the film, resulting generally of several larger domains (Figure 8, images b1 and b2) having a high tendency to interact and to form a film (without recompressing) where the 3D transformations were still present.

**Optical Properties of POAS LB Films.** The obtained results suggested that, from a practical point of view, a good compromise of surface deposition pressure is comprised in the range  $25\text{--}35 \text{ mN m}^{-1}$ . In fact, dealing with the presence of breaks, collapses, or other defects, as well as to the stability at the air/water interface or to the reliability of the deposition, the

indicated range seemed to be the optimum one. Exceeding the surface pressure of  $35 \text{ mN m}^{-1}$  the possibility of observing the presence of 3D transformations at the air/water interface due to collapses, was very high and the film stability decreased as well. Furthermore, surface pressures less than  $25 \text{ mN m}^{-1}$  underlined the possibility of depositing films that have larger breaks, as also observed using BAM. The presence of these defects disturb the properties and the quality of the film polymer. Therefore, a surface deposition pressure of  $25 \text{ mN m}^{-1}$  was chosen to analyze the electrooptical properties of POAS LB films.

The optical spectrum of the POAS EB LB film is shown in Figure 9 (thick line): it reflects the typical spectra of polyaniline emeraldine base.<sup>46,47</sup> The optical absorption at 619 nm (2.0 eV) in the emeraldine base could be due to a  $n\text{--}\pi^*$  transition from the nonbonding nitrogen lone pair to the conduction ( $\pi^*$ ) band or as a result of a neutral exciton (bound electron–hole pair). However, as indicated by Ray et al.,<sup>46,47</sup> it is possible to speculate that although the 2.0 eV transition is forbidden by symmetry in the perfect system (band calculation), the disorder in the amorphous POAS LB films<sup>25,48</sup> can be expected to lead to nonbonding states in the gap and to turn on the transition

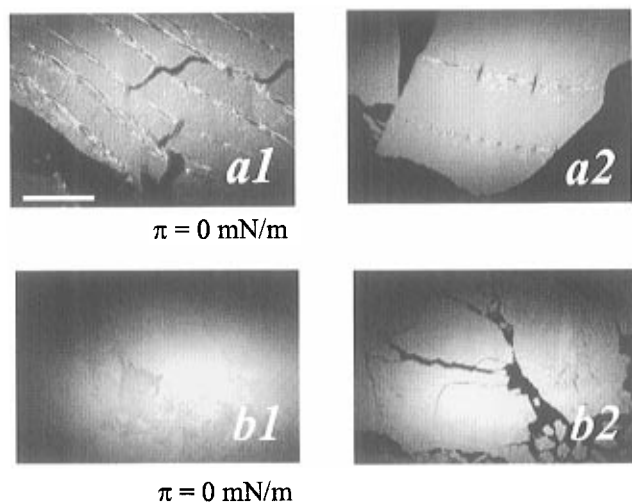


**Figure 8.** BAM images of the POAS EB (a1 and a2) and of the POAS ES (b1 and b2) Langmuir films morphology immediately after the opening of barriers when the maximum compression is reached: the surface pressure decreased sharply to 0 mN m<sup>-1</sup> (see text), and it was possible to confirm that the 3D transformations occurred, namely collapses, were irreversible.

(intrachain and interchain) from the nonbonding state to the conduction band, thus implying that the 2.0 eV absorption has its origin in the nonbonding lone-pair state. The peak near 315 nm (3.93 eV) is produced by  $\pi$ - $\pi^*$  interband transitions. These two broad transitions characterize the emeraldine base form of the POAS LB film and makes it blue in color. When a doped POAS LB film was made new absorption bands arose near to 870 nm (1.42 eV), 352 nm (3.52 eV), and 450 nm (2.75 eV; Figure 9, thin line). The last two peaks formed a broad band and underlined the presence of polarons in the POAS system.<sup>3,25,46,47</sup> In fact, there is an emergence of a new band near 450 nm and a red-shift in the band from 315 to 352 nm. The peak at 450 nm is very similar to that found for the overoxidation of the monomer and demonstrates the polarons generation in the POAS system. The band at 870 nm is due to the defect incorporated during the doping process or to the delocalized free electron state of POAS molecules in the LB film.

Moreover, the intensities of the bands distinctly increased with the increase in the deposited layers on the quartz plate.

Further, it was assessed that the increase of the subphase molarity, which corresponds to a decrease in pH, modified the electrooptical properties from the EB form to the ES form of POAS LB films conducting polymer (data not shown).

The protonation of POAS, which form the emeraldine salt, led to a dramatic change in conductivity, from 10<sup>-10</sup> S cm<sup>-1</sup> for unprotonated polymer to 0.1 S cm<sup>-1</sup> when doped by a 1 M HCl aqueous solution.<sup>25</sup> In fact, the highest conductivity of POAS was achieved when the doped polymer was further exposed to a 1 M HCl solution. Therefore, it is possible to state that POAS LB films can readily be obtained in the doped state and that the dopant level can be enhanced by subsequent doping in an 1 M HCl solution.<sup>25,26</sup>

The optical bandgap of POAS EB and of POAS ES forms was estimated to be 3.8 and 2.7 eV, respectively (also see Table 1). These values are in agreement, as order of magnitude, with the polyaniline polymer system.<sup>2,3,13</sup> Generally, the bandgap governs the intrinsic electrical and optical properties of the polymer,<sup>2,3</sup> and its reduction underlines the increase of intrinsic conductivity of the conjugated polymer due to the doping process, as observed for the undoped (EB) and the doped (ES) forms of the POAS system.

## Conclusions

In this work the Langmuir-Blodgett technique has been successfully applied to obtain ultrathin films of POAS conducting polymer. The performed investigation emphasized that the inclusion of an HCl dopant in the polymer backbone, which occur during the film formation, was able to change its structure, thus inducing a different organization of the POAS molecules at the air/water interface, and to modify the electrooptical properties. Although it has been impossible to know the real organization of the polymer at the air/water interface, the investigation carried out made it possible to speculate about the formation of POAS LB films and to study some main features linked to the doping process.

The study at the air/water interface suggested that the close association of the counterion (Cl<sup>-</sup>) with the POAS polymer

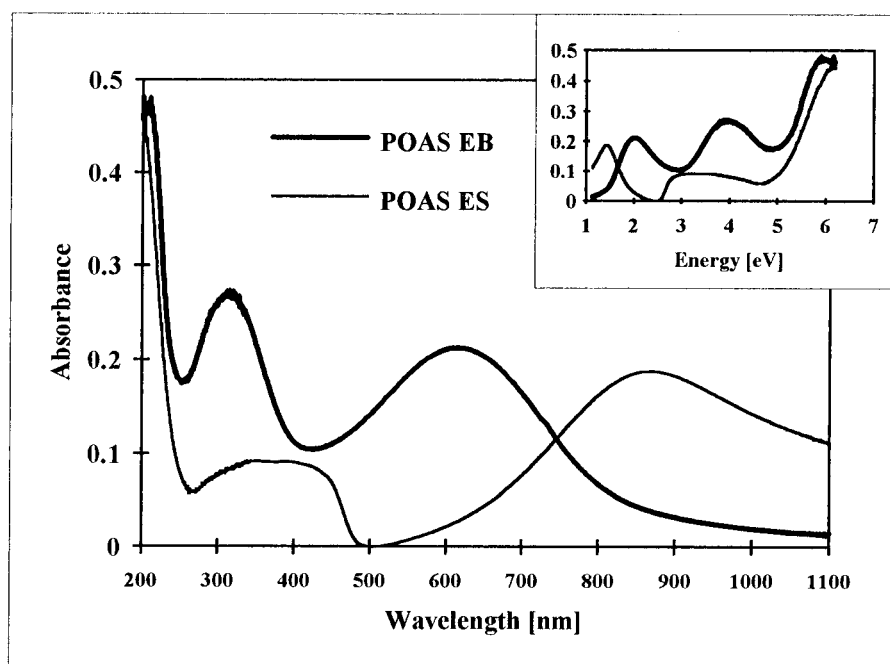


**Figure 9.** UV-vis-near-IR absorption spectra of POAS EB and of POAS ES LB films deposited onto a quartz plate. The surface deposition pressure was 25 mN m<sup>-1</sup>, and the films were 20 layers thick. The inset reports the film absorption as a function of photon energy. By the analysis of these spectra it was possible to estimate the bandgap of the polymer in its undoped and doped forms.

backbone distorted the microstructure of the polymer to accommodate this extra mass. In fact, the doping process, in addition to the protonation of the imines nitrogens in the POAS polymer, requires the conjugate base of the doping acid to act as a counterion to maintain the electroneutrality in the doped polymer. The Brewster angle microscopy allowed one to follow the Langmuir film formation and to display its morphology, as well as to correlate the 2D/3D transformations with the shape of the  $\pi/A$  isotherms simultaneously recorded. In fact, the BAM images revealed the presence of breaks or defects and displayed the nucleation and the growth of 3D structures which occurred during the continuous overcompression of the 2D film beyond the limiting densities of packing, namely collapses. Likewise, it has been found that the interactions of the film with the aqueous subphase had a stronger influence on the organization of the molecules and on the morphology of the 2D–3D transformations.

The process adopted to dope the polymer, i.e., by utilizing a HCl-acidified solution at subphase, has been proved reliable and effective, although the highest conductivity was reachable by exposing the deposited film to a 1 M HCl solution. In addition, the analysis at the air/water interface and the QCM measurements permitted one to evaluate the deposition reliability as well as to adopt a suitable deposition surface pressure. The optical study allowed the confirmation of structural changes induced by the inclusion of dopant and to assess the optical properties. In fact, the modification of the optical spectra, as underlined by polarons and bipolarons formation, and the decrease in the bandgap, from POAS EB to POAS ES LB films, indicated the increase of an intrinsic conduction of POAS polymer due to the chloride doping process which occurred during the film's formation.

Therefore, the results obtained in this work demonstrate that the Langmuir–Blodgett technique is adequate to form and to deposit in a controlled way the POAS polymer organized in ultrathin films. Furthermore, the possibility of knowing and/or controlling parameters such as the stability of the film, the packing degree of the molecules organized in film or the morphological features allow one to overcome designing problems crucial for the preparation of homogeneous and highly ordered layered structures with a low concentration of defects. In fact, these features make it possible to design molecular assemblies of POAS conducting polymer aimed at practical purposes, such as molecular devices, electrochromic displays or special coatings.

**Acknowledgment.** The authors are grateful to Dr. P. Facci and Dr. V. Erokhin for their criticisms during the writing of this paper. Thanks also to Mr. F. Nozza, Miss C. Rando, and Mr. A. Rossi for their technical support. Financial support by the E.L.B.A Foundation and the University of Genoa is gratefully acknowledged.

## References and Notes

- (1) Skotheim, T. A., Ed. *Handbook of conducting polymers*; Dekker: New York, 1986.
- (2) Maiti, S.; Rahman, S.; Kundu, S. *Bull. Electrochem.* **1992**, 8 (11), 556–573.
- (3) Patil, A. O.; Heeger, A. J.; Wudl, F. *Chem. Rev.* **1988**, 88, 183–200.
- (4) Ray, A.; Asturias, G. E.; Kershner, D. L.; Richter, A. F.; MacDiarmid, A. G.; Epstein, A. J.; *Synth. Met.* **1989**, 29, E141–E150.
- (5) Ray, A.; Richter, A. F.; MacDiarmid, A. G.; Epstein, A. J. *Synth. Met.* **1989**, 29, E151–E156.
- (6) Huang, W. S.; MacDiarmid, A. G.; Epstein, A. J. *J. Chem. Soc., Chem. Commun.* **1987**, 1784.
- (7) Epstein, A. J.; MacDiarmid, A. G. In *Electronic properties of conjugated polymer*; Kuzmany, H., Mehring, M., Roth, S., Eds.; Springer-Verlag: Berlin, 1989.
- (8) Langner, J. J. *Synth. Met.* **1990**, 36, 35.
- (9) Pouget, J. P.; Józefowicz, M. E.; Epstein, A. J.; Tang, X.; MacDiarmid, A. G. *Macromolecules* **1991**, 24, 779–789.
- (10) Echigo, Y.; Asami, K.; Takahashi, H.; Inoue, K.; Kabata, T.; Kimura, O.; Ohsawa, T. *Synth. Met.* **1993**, 55–57, 3611–3616.
- (11) Nešpurek, S.; Sworakowski, J. *IEEE Eng. Med. Biol.* **1994**, Feb/March 45–57.
- (12) Sangodkar, H.; Sukeerthi, S.; Srinivasa, R. S.; Lal, R.; Contractor, A. Q. *Anal. Chem.* **1996**, 68, 779–783.
- (13) Ramanathan, K.; Ram, M. K.; Malhotra, B. D.; Surya, A.; Murthy, N. *Mater. Sci. Eng.* **1995**, C3, 159–163.
- (14) Coklin, J. A.; Anderson, M. R.; Reiss, H.; Kaner, R. B. *J. Phys. Chem.* **1996**, 100, 8425–8429.
- (15) Wessling, B. *Adv. Mater.* **1994**, 6, 226–227.
- (16) Gustafsson, G.; Cao, Y.; Treacy, G. M.; Klavetter, F.; Colaneri, M.; Heeger, A. J. *Nature* **1992**, 357, 477–478.
- (17) Misra, S. C. K.; Ram, M. K.; Pandey, S. S.; Malhotra, B. D.; Chandra, S. *Appl. Phys. Lett.* **1992**, 61, 1219–1221.
- (18) Gardner, J. W.; Bartlett, P. N. *Sensors Actuators A* **1995**, 51, 57–66.
- (19) Mattoso, L. H. C.; Mello, S. V.; Riul, A.; Oliveira, O. N.; Faria, R. M. *Thin Solid Films* **1994**, 244, 714–717.
- (20) Porter, T. L.; Dillingham, T. R.; Lee, C. Y.; Jones, T. A.; Wheeler, B. L.; Caple, G. *Synth. Met.* **1991**, 40, 187–196.
- (21) Maeda, Y.; Katsuta, A. *Synth. Met.* **1993**, 58, 131–135.
- (22) Gonçalves, D.; Bulhões, L. O.; Mello, S. V.; Mattoso, L. H. C.; Faria, R. M.; Oliveira, O. N. *Thin Solid Films* **1994**, 243, 544–546.
- (23) Shaolin, M.; Caifen, X. *Synth. Met.* **1993**, 59, 243–247.
- (24) Kang, E. T.; Neoh, K. G.; Tan, K. L.; Wong, H. K. *Synth. Met.* **1992**, 48, 231–240.
- (25) Ram, M. K.; Carrara, S.; Paddeu, S.; Maccioni, E.; Nicolini, C.; *Langmuir*, in press.
- (26) Ram, M. K.; Carrara, S.; Paddeu, S.; Nicolini, C. *Thin Solid Films*, in press.
- (27) Ulman, A. *An introduction to ultrathin organic films: from Langmuir–Blodgett to Self-Assembly*; Academic Press: Boston, 1991.
- (28) Blodgett, K. B.; Langmuir, I. *Phys. Rev.* **1937**, 51, 964.
- (29) Roberts, G. *Langmuir–Blodgett films*; Plenum Press: New York, 1990.
- (30) Hönig, D.; Möbius, D. *J. Phys. Chem.* **1991**, 95, 4590–4592.
- (31) Hönig, D.; Möbius, D. *Thin Solid Films* **1992**, 210/211, 64–68.
- (32) Hénon, S.; Meunier, J. *Thin Solid Films* **1992**, 210/211, 121–123.
- (33) Langmuir, I.; Schaefer, V. J. *J. Am. Chem. Soc.* **1938**, 60, 1351–1360.
- (34) Sauerbray, G. Z. *Z. Phys.* **1959**, 155, 206–212.
- (35) Guilbault, G. G.; Jordan, J. M. *Analytical uses of piezoelectric crystals: a review*; CRC Press: London, 1988; Vol. 19, pp 1, 1–28.
- (36) Pandey, S. S.; Misra, S. C. K.; Malhotra, B. D.; Chandra, A. S. *J. Appl. Polym. Sci.* **1992**, 44, 911.
- (37) Annapoorni, S.; Sundaresan, N. S.; Pandey, S. S.; Malhotra, B. D. *J. Appl. Phys.* **1993**, 74, 2109.
- (38) Facci, P.; Erokhin, V.; Nicolini, C. *Thin Solid Films* **1993**, 230, 86–89.
- (39) Ahuja, R. C.; Caruso, P. L.; Hönig, D.; Maack, J.; Möbius, D.; Overbeck, G. A. In *Microchemistry*; Masuhara, H., et al., Eds.; Elsevier Science B. V.: Dordrecht, 1994, 211–223.
- (40) Hönig, D.; Overbeck, G. A.; Möbius, D. *Adv. Mater.* **1991**, 4, 419–424.
- (41) Hönig, D.; Möbius, D. *Chem. Phys. Lett.* **1992**, 195, 50–52.
- (42) Jenkins, F. A.; White, H. E. *Fundamental of optics*, 4th ed.; McGraw-Hill Book Co.: New York, 1987; Chapter 24.
- (43) Mello, S. V.; Mattoso, L. H. C.; Santos, J. R.; Gonçalves, D.; Faria, R. M.; Oliveira, O. N. *Electrochim. Acta* **1995**, 40, 12.
- (44) Cheung, J. H.; Rubner, M. F. *Thin Solid Films* **1994**, 244, 990.
- (45) Angelova, A.; Vollhardt, D.; Ionov, R. *J. Phys. Chem.* **1996**, 100, 10710–10720.
- (46) Kim, Y. H.; Foster, C. M.; Chiang, J. C.; Heeger, A. J. *Synth. Met.* **1989**, 29, E285–E290.
- (47) Kim, Y. H.; Phillips, S. D.; Nowak, M. J.; Spiegel, D.; Foster, J. M.; Yu, G.; Chang, J. C.; Heeger, A. J. *Synth. Met.* **1989**, 29, E291–E296.
- (48) The amorphous nature of POAS LB film has been verified by an X-ray small angle scattering analysis presented in a previous work.<sup>25</sup>